Bull. Inst. Chem. Res., Kyoto Univ., Vol. 67, No. 2, 1989

Time-Division Integrated Light Scattering Photometer 1. Its Construction and Performance

Yoshisuke TSUNASHIMA,*[1)] Norio NEMOTO,* and Michio KURATA**

Received May 26, 1989

Described is a light scattering instrument facilitating simultaneous measurement of angular distribution of the light scattered from transient events at intervals of as short as 1 ms and discussed is its performance. In each interval, the scattered light is gathered simultaneously at 30 angles in the range 8° to 150°, and its distribution is imaged through optical fibers on a detector of a linear array of 512 self-scanning photodiode elements and is transferred to a direct-access memory under the controll of a microcomputer of a 16 bit CPU, a 10 MHz internal clock, and 1.2 MB memory. Data are presented for a solution of styrene-butadiene diblock copolymer in *n*-decane, showing rapid fluctuation of the structure formed in this solution.

KEY WORDS: Light Scattering/ Time-Division Spectroscopy/ Rapid Scan Photometer/ Linear Photodiode Array Detector/

INTRODUCTION

In this paper we present a new type of light scattering instrument, time-division integrated light scattering (TIDILS) photometer, which allows us to follow succesive alteration of the angular distribution of the light intensity scattered from solutions at intervals of as short as 1 ms.[2)] This photometer can integrate simultaneously but individually the scattered light at 30 angles which cover the scattring angle over 8° to 150°. The scattered light signal gathered at each angle passes through a quartz window, which is put in the bath wall, and then through an optical fiber and finally reaches the specified area of an intensified PCD (Plasma-Coupled Device) linear detector of 512 monolithic self-scanning silicon photodiode elements. The detector is scanned at a maximum rate of 500 ns per elements. The zero target lag and low blooming of this detector facilitates both rapid time resolution and fine angular resolution of the intensity distribution of the light scattered from transient phenomena or time-resolved phenomena.

OUTLINE OF TIDILS SYSTEM

A simplified block diagram of the TIDILS system is shown in Figure 1. Essensially, the TIDILS system consists of an optical system for measuring the scattered light intensity at multiangles, an intensified linear photodiode detector unit, a temperature/concentration jump system, and the microcomputer-based multichannel analysis network which includes a PC–98 16–bit CPU, I/O digital interface circuits

* 綱島良祐, 根本紀夫 : Laboratory of Fundamental Material Properties, Institute for Chemical Research, Kyoto University, Uji, Kyoto-fu 611.
** 倉田道夫 : Mitsubishi Gas Chemical Co. Inc., Katsushika-ku, Tokyo 125.

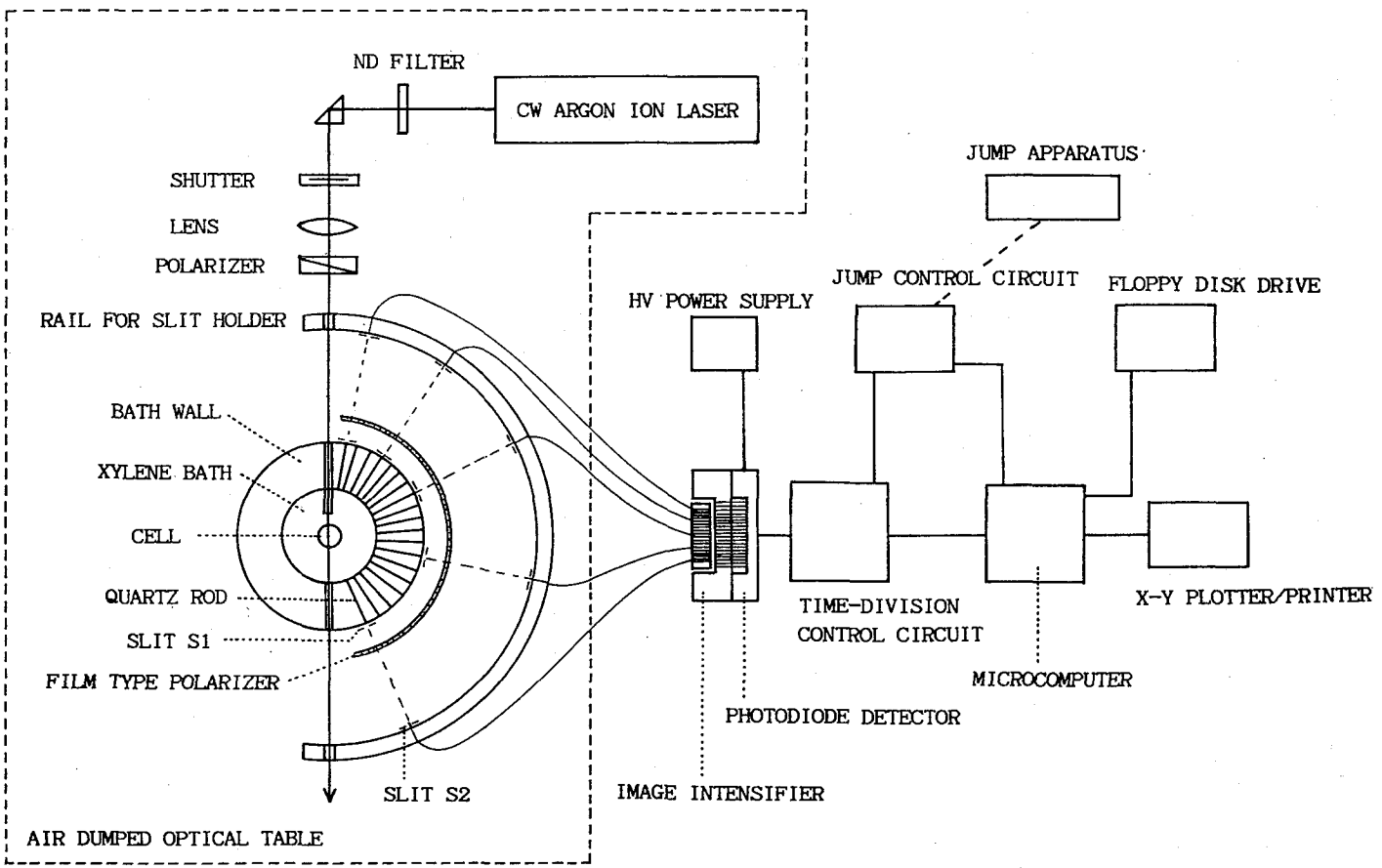

Fig. 1. Block diagram of the time-division integrated light scattering apparatus

(time-division and JUMP circuits), a signal/data processing program package and peripherals of a CRT color display, a X-Y plotter/printer, and a dual-drive floppy disk device. The optical system and a light source are mounted on an optical table with air suspension vibration isolator.

The light source is a single-frequency 488 nm line emitted from a CW argon ion laser (Spectra-Physics, Model 2020-03/2560/2210, 3W) equipped with an air spaced etalon. Passing through a rotatable neutral density filter (0–100% attenuation) and a remote controlled electric shutter, the laser beam is focused with an achromatic collimating lens on the central position of a temperature-controlled xylene bath, at which position the radial center of a measuring cell is set precisely. An air spaced double prism polarizer of a modified Gran-Foucault design, which is inserted between the lens and the bath, transmits only a vertical component of the linear polarized laser light. The cell is a selected NMR cylindrical glass tube of 12 mm outer diameter (0.5 mm thickness) with a ground glass stopper. It is hung from a precision chuck.

The scattered light from a sample solution in the cell is detected only at the specified 30 angles in the range of 8°–150°, each direction being determined with a pair of slits S1 and S2 (300μm width) set radially 200 mm apart each other. At each angle, a quartz rod of which cross sections (edges) are optically polished is put radially in the bath wall and serves as a window for guiding the specified scattered light to an polished edge surface of the optical fiber. Another edge of the optical fiber is attached to the photocathode input window of an image intensifier in the following way: the optical fibers arranged at 30 scattering angles are bundled and molded together into a linearly arranged packet, following which the packet edge is polished optically and then made fast contact with the photocathode window of the image intensifier. The scattered light thus introduced into the intensifier is multiplied about 10^4 times at maximum and the intensity distribution profile is imaged on a 512 channels linear photodiode detector that is fiber-optically coupled to the image intensifier. A film type polarizer inserted between the slits S1 and S2 allows to transmit only a vertical component of the scattered light (Vv component) to the detector.

Since the intensity stored on the detector relates linearly to the integration period or exposure time of the detector, the exposure time to the light must be adjusted to the time constant of measuring phenomena and to the intensity scattered from sample solutions. Once the exposure time elapses, the detector starts to scan the stored signals at a rate of 500 ns per element. The intensity signals are digitized and transferred to a direct-access data memory, following which the acquired intensity distribution profile of the scattered light is displayed on the CRT screen as intensity vs. channel data. After receiving a required processing, the data are read out to the CRT display or a peripheral hard-copy device of X-Y plotter and stored on a floppy disk. In this process, the time-division control circuit serves as the TIDILS system controller. It powers the intensifier with a high voltage DC (0–1.0 KV variable) power supply, collects and processes the scattered light signals gathered on the detector, stores them on a direct-access data memory, performs signal averaging of

multiscans, and controls TIDILS data acquisition and processing. The microcomputer controls all the operating programs necessary for this system. It sets initial conditions of TIDILS measurements, displays the acquired data profiles, performs arithmatic operation on data, reads out raw or processed data to the CRT display or the X-Y plotter, and writes them on the floppy disk.

The JUMP circuit is usuful for temperature/concentration jump measurements where rapid changes are introduced into measuring solutions. The circuit controls all the data acquisition and processing performed on jump instruments such as a stopped-flow apparatus.

In what follwos, we describe more in detail (a) the cell housing and receiving optical system, (b) the intensified TIDILS detector and its rapid scan control circuit, and (c) the data acquisition/processing network.

CELL HOUSING AND RECEIVING OPTICAL SYSTEM

The cell housing and receiving optical system facilitate simultaneous multiangle detection of the scattered light under high precision angular regulation. A measuring glass cell is immersed in refractive index matching liquid (xylene) in the sampling bath.[3] Xylene is optically cleaned and its temperature is controlled to within $\pm 0.02°C$ through temperature-controlled liquid (water) which is circulating around a channel bored in the bath wall. The bath wall has 30 pieces of window holes, bored through radially as follows: 4 pieces at 8°–20° at intervals of 4° and 26 pieces at 25°–150° at intervals of 5°, into which holes 2 mmϕ quartz rods of optically polished edges are molded. In the incident ($\theta=0°$) and exit ($\theta=180°$) directions of the laser light, another but longer quartz rods are also molded. The long entrance quartz rod (6 mmϕ, 60 mm long),[4,5] which projects into xylene as far as 25 mm in front of the cell, has the advantage of reducing significantly the stray light and of enhancing the reproducibility of the measured intensity.

A pair of slits S1 and S2 (300 μm width $\times$ 1.0 mm hight) at each angle regulate precisely the scattering volume in the sample solution: the first slit S1 is set just behind the quartz rod and the second slit S2 on a X-Y adjustable slit holder that is mounted on a semicircular rail of 300 mm radius. This rail is set coaxially with the bath as well as the cell. The distance R between S1 and S2 is 200 mm. This slit alignment offers an advantage over conventional static light scattering photometers: if the slits are exchanged with a pair of pinholes under the coherence condition that $d_1 d_2 \leqq 2.44 R\lambda_0$,[6] this photometer works as a dynamic light scattering spectrometer. Here d_1 and d_2 are the pinhole diameters of S1 and S2, respectively, and λ_0 the wavelength of the incident light in vacuum.

Optical fibers of 1 m long (clad radius 800 μmϕ, core radius 700 μmϕ) transfer the observed scattered light at S2 slit to the photocathode of an image intensifier (Hamamatsu Photonics K.K., Model V1366). One edge of these fibers is molded individually into a piece of black insulater and is optically polished so as to make its cross section rectangular to the fiber axis, and put on the center of each S2 slit. 30 pieces of another edges are aligned and molded together into a block of black

insulator (a fiber holder, its cross section is 10 mm × 40 mm) and are polished optically. This 30 pieces of optical fiber array forms a cross section of ca. 800 μm (height) × 25 mm (width), which size is nearly equal to the effective diameter of photocathode surface of the image intensifier V1366 (25 mmϕ). A 512 channels linear photodiode detector (Hamamatsu Photonics K.K., Model S2301–512Q) has also a photosensitive area of 2.5 mm (height) × 28 mm($\simeq$50 μm × 512, width). Thus a series of precise optical coupling of the fiber holder with the image intensifier and with the photodiode detector provides the exact image of the scattered light distribution profile on the detector.

INTENSIFIED TIDILS DETECTOR AND ITS RAPID SCAN CONTROL CIRCUIT

The intensified TIDILS detector features the high sensitivity of image detector. It is a photon counting imager coupling fiber-optically the V1366 image intensifier on to the S2301-512Q linear photodiode detector/C2325–28S driver/amplifier circuit (Hamamatsu Photonics K.K.). The image intensifier is an evacuated glass envelop in which a Multi-Alkali photocathode (photon-to-electron converter), an electron lens, a microchannel plate (MCP, electron intensifier) and a phosphor screen (electron-to-photon converter) are sealed. A fiber optic plate attached behind the phosphor screen works as a window which makes access to the detector easy. When a photon image is implinged on the photocathode, the cathode emitts photoelectrons corresponding to the photon image. The photoelectrons focus into image on the MCP input surface through the electron lens. The MCP is a two-dimensional electron multiplier made of a glass plate of 1.5×10^6 pieces of channels (micro glass capillaries of 12 μmϕ), in which channel a single electron results in emit more than thousands of secondary electrons due to its multiple collisions with the channel wall. The multiplied electrons then impinge upon the phosphor screen under a high electron field, in which screen they are coverted again into an optical image. The input signal intensity is thus intensified up to 4×10^4 times in this process, which value depending on the voltage supplied on the intensifier.

The linear photodiode detector is a self-scanning image sensor of the monolithic integrated circuit. It is constructed from a linear array of 512 silicon photodiode elements, a PCD shift register (bipolar static type self-scanner) and switching transistors for addressing the photodiode elements. This detector features zero target lag, low blooming, high ouptut linearity/uniformity, wide dynamic range, and long integration time stability. In the photodiode array, 512 diffused *p*-type silicon regions of 50 μm center-to-center spacing × 2.5 mm hight are aligned in a row in *n*-type silicon substrates. When photon signals are applied, the charges are generated in these two regions, and then collected and stored on the associated *p-n* junctions capacitance during the integration period of the detector. Following the period, the scan is initiated by a start pulse and the PCD shift register transfers sequentially an addressing pulse (TTL compatible) along the chain driven by a synchronized three pulse clock. Each output pulse from the PCD shift register is then fed to the base electrode of each *p-n-p* switch in the video circuit, which has a charge-amplifier of current

integration type. With this circuit, the charge-amplifier is reset to ground prior to address each photodiode multiplex switch. Immediately after the switch is on, the signal charges flow into capacitors in the integration circuit. In this sensor, the photodiode array acts as the emitters in the transistors and operates in the charge storage mode. Therefore the phododiode outputs are proportional to the illumination intensity multiplied by repeated scanning period.

The maximum operating frequency of 2 MHz guarantees that the image on the detector can be completely erased in one read-out cycle at this frequency and that the detector shows really no target lag, where the lag is defined as the persistence of optical information on the detector from one integration to the next. Blooming, defined as the spreading of a strong optical signal from one detector element to adjacent elements, hides and degrades seriously resolution of weak signals in the presence of strong ones. However, this S2301–512Q detector minimizes the blooming by adopting the p-type diffused region arrays in the detector geometry. This geometry ensures low dark leakage current overlapped on the optical signal. Moreover, the detector shows high output linearity and uniformity, as characterized by the linearity between the output charge (pC) vs. exposure (lux. sec) relation over the range 10^{-2} to 20 pC. This characteristics ensures the wide dynamic range of the detector, which range being determined by the ratio of the largest and smallest signals for which the detector is linearly proportional to the input signal intensity. This characteristics also facilitates a fully realization of the 12-bit (4096:1) conversion gain of the analog-to-digital (AD) converter.

DATA ACQUISITION/PROCESSING NETWORK

With a 16-bit CPU microcomputer of a 10 MHz internal clock, 1.152 MB memory and a dual-drive 5-inch floppy disk of 1 MB memory area, the control circuit in the present TIDILS data acquisition/processing network operates at a scan rate of 2 μs per detector element under optimum conditions. This scanning rate means that acquisition of the desired intensity distribution profile takes only 1.024 ms for the present 512-element detector. A background (i.e., dark current) distribution profile is measured in advance and can be stored as a reference. Once obtained, this background profile is subtracted from any series of subsequent light scattering measurement. Instant display of the intensity distribution profile thus processed can be done in real time.

Figure 2 shows the genelarized TIDILS data acquisition diagram. First, this data acquistion pattern is roaded on the microcomputer through keyboard commands. When a start pulse for measurement is generated on the intensified TIDILS control circuit through the computer or via the JUMP circuit, the system clock is set on $t=0$ and the TIDILS measurement starts. At $t=t_1$, the detector is open to the scattering light and starts to gather the light intensity for Δt_1, and then closed. During the waiting time of Δw_1, the intensity signal charged on the detector channels are all scanned and transferred to the direct-access memory (DAM) area of the computer, and the detector is again ready to accept the next data acquisition.

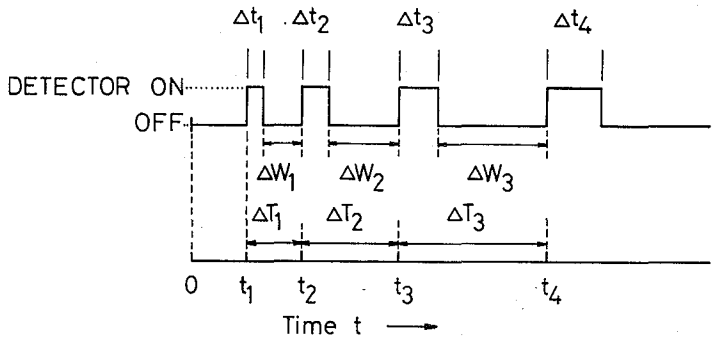

Fig. 2. Data acquisition diagram performed on the time-division control circuit. t_i: the time when the detector starts to gather the scattered light; Δt_i: the integration period during which the detector gathers the scattered light, i.e., the exposure time of the detector; ΔT_i: the time interval of a single data acquisition; Δw_i: the waiting time of the detector (including the data processing time).

At $t=t_2$, the detector is open and starts again to gather the intensity signal for Δt_2, and then the signal is transferred to DAM, and so on. Sequential data acquisition at $t=t_1, t_2, t_3, \cdots, t_i$ for $\Delta t_1, \Delta t_2, \Delta t_3, \cdots, \Delta t_i$, respectively, thus offers the time-division intensity distribution of the scattered light from the measuring system. A simplest pattern of various data acquisition is that $\Delta t_1=\Delta t_2=\cdots=\Delta t_i$ with $\Delta T_1=\Delta T_2=\cdots=\Delta T_i$ (Equal exposure time of the detector at equal intervals). During the measuremet, a part of the incident light is detected throught a PIN silicon photodiode (S1366-8BK, Hamamatsu Photonics K.K.) to monitor the intensity fluctuation of the incident light. The signal output of the monitor is stored on a microcomputer DAM area.

INSPECTIONS OF OPITICAL SYSTEMS AND DATA ACQUISITION/PROCESSING SYSTEMS

OPTICAL COUPLING OF ALIGNED OPTICAL FIBERS WITH THE INTENSIFIED DETECTOR AND RESOLUTION POWER OF THE SCATTERED LIGHT

Figure 3 shows channel number dependence of the scattered light intensity from aqueous suspensions of polystyrene-latex particles of 91 nm nominal diameter (Dow Chemicals). In this case, only three measuring windows corresponding to angles at 30°, 60°, and 90° were opened to the scattered light for 500 ms, and the gathered intensity signal was displayed without processing the background subtraction. As is clearly shown in the figure, three intensity peaks appear at the channel numbers corresponding to these angles. The other channels, which were covered from the scattered light, do not show any remarkable intensity peak but give, independent of channels, a constant amount of weak background signal which works as the reference intensity of this experiment. The background comes mainly from the dark signal from this image intensified detector. Its amounts were however constant, about 8% in a relative intensity unit, and were reproducible at each experiment, which feature allowed this background to be precisely removed by subtraction from any series of subsequent measurements under exactly the same condition that the

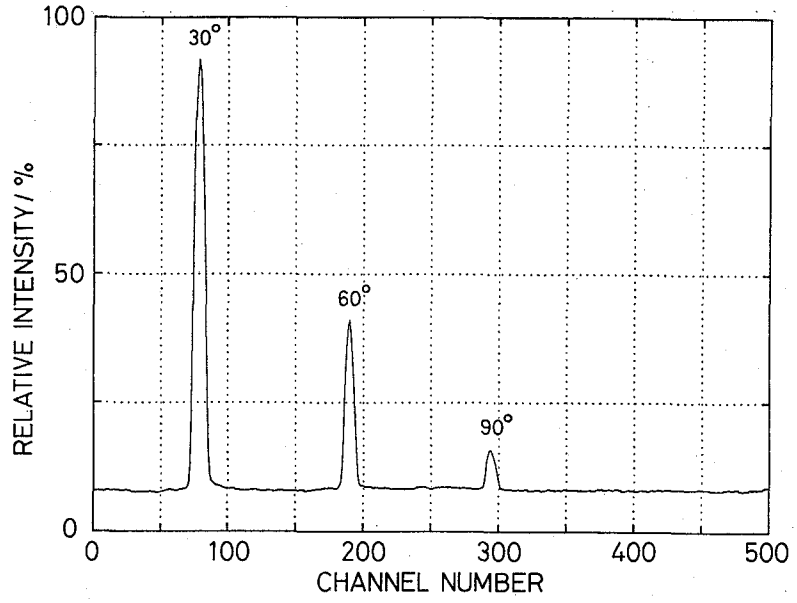

Fig. 3. Relations between the intensity profiles of the scattered light at three angles (30°, 60°, and 90°) and the channel numbers of the photodiode detector. The scattered light from aqueous suspensions of polystyrene-latex particles was measured at 25°C for 500 ms.

background was measured.

The intensity peaks appeared at 30°, 60°, and 90° were symmetric in shape and their spread was limitted to within 8 ± 1 channels on both sides of their central channel, i.e., to within 17 ± 1 channels, independent of the strength of the scattered light. The blur or spreading of this intensity signal (blooming) from these channels to adjacent outer channels was never observed. This fact assured that the scattered intensity signal at each scattering angle was stored rigidly on the specified channel numbers of the detector. Morever, the channel numbers between central channels for the intensity peak at 30°, 60°, and 90° were counted to be 108 ± 2. This number indicated that the channel numbers assigned to a single optical fiber was to be 18 (=108/6), since we set 6 pieces of optical fibers between 30° and 60° and between 60° and 90°, respectively. The number 18 agreed compretely with the above-mentioned channel numbers 17 ± 1, which was obtained from the peak width at each scattering angle. Completely the same results were obtained for the intensity signal at the other scattering angles. These results confirmed that the polished fiber ends for specified 30 scattering angles were aligned on the intensifier surface in order of angle and were coupled precisely with the intensified detector. It should be noted that the channel number 18 per single optical fiber obliges us to measure simultaneously the scattered light at 28 angles, not at 30 angles. To measure in the lower angle region of 8°–140°, we must slide the optical fiber holder a little bit to the central portion of the intensifier surface. In this case, the assignment of the channel numbers to the scattering angles is made automatically on the microcomputer.

MEASUREMENTS OF FLUORESCENCE AND OF SCATTERING FROM BENZENE

Fluorescence and scattering from benzene must be measured to test the performance of this TIDILS photometer. Fluorescence intensity from a dilute fluorescent solution is proportional to the scattering volume and is independent of the scattering angle θ. The intensity $I(\theta)$ multiplied by $\sin\theta$ should be constant over all the scattering angles if the optical systems and the measuring cells are precise in geometry and optics. Angular distribution of the scattered light from pure solvents such as benzene and carbon tetrachloride should also give a constant value in terms of $I(\theta)\times\sin\theta$ over all the scattering angles measured, if the photomener is under proper condition geometrically and optically. If not, the distribution gives information about an amount of the stray light, abnormal scattering, improper usage of optical elements, and hidden experimental mistakes.

Our goal in these experiments is to investigate (1) whether the optical sensitivity is equal to all the detector elements, (2) whether the scattering volumes or the scattering angles are determined correctly by the two slits, and (3) how many amount of the stray light appears at lower scattering angles such as below 20°.

The angular distribution of fluorescence intensity was first measured with a dilute fluorescein-cyclohexanol solution, which solution was filtered through a 0.50 μm (pore size) Millipore filter. The detector gathered the fluorescence excited by the incident 488 nm line. In this situation, a yellow sharp cut filter (SC–52, Fuji Film), which was set just on the outer margin of first slits in a radial rank, functioned as a filter which transmitted only the light of longer wavelength than that of the scattered light, 488 nm. Next, the angular distribution of the scattered light from benzene (spectrograde, Nakarai Tesque) was measured, benzene being filtered into a 12 mmϕ cell through a Millipore filter of 0.22 μm pore size. The exposure time of the detector was 500 ms in both measurements and the sample liquids were controlled at 25.00 ± 0.02°C.

Prior to the present measurements, we have performed the correct regulation of 30 scattering angles by carrying out the dynamic light scattering measurements at these 30 angles with aqueous suspensions of polystyrene-latex particles of 91 nm diameter, in which measurements the slits were all exchanged by pinholes of 100–300 μm diameter. We have concluded that this angular regulation satisfied the item (2), which conclusion was guaranteed by the fact that the values of $I(\theta)\times\sin\theta$ were constant to within $\pm5\%$ over 8°–150° in the present fluorescence measurements. We therefore assumed that the item (1) was satisfied to within experimental error and that the amounts of the stray light at given low scattering angles (the item (3)) could be estimated to be an excess $I(\theta)\times\sin\theta$ value over the average at higher scattering angles. We thus corrected the scattered light intensity at lower angles by subtracting the estimated stray light from the raw data.

In Figure 4 and 5, the intensity distribution of the scattered light from benzene thus corrected is plotted as a function of the detector channel number and of the scattering angle, respectively. The detector exposure time was 500 ms as described

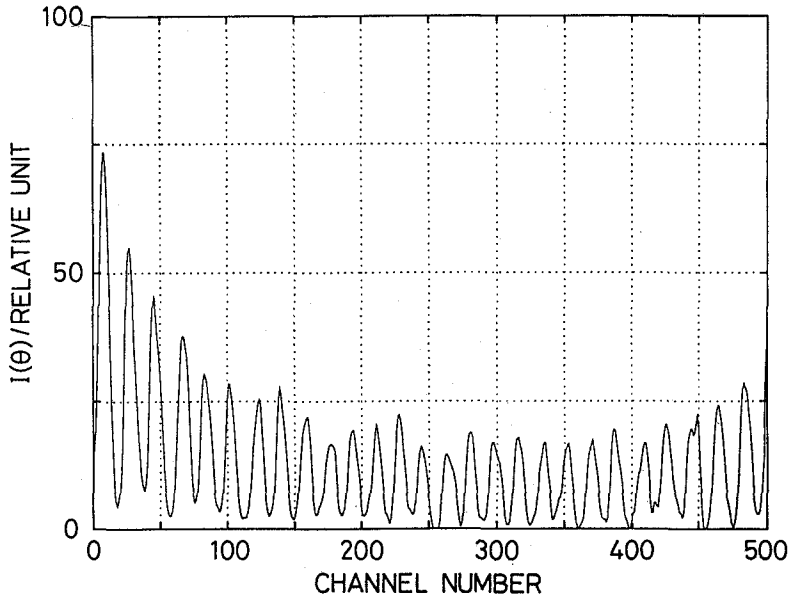

Fig. 4. Intensity distribution of the scattered light from benzene plotted against the channel numbers of the detector. The measurement was made at 25°C with the exposure time of the detector Δt=500 ms.

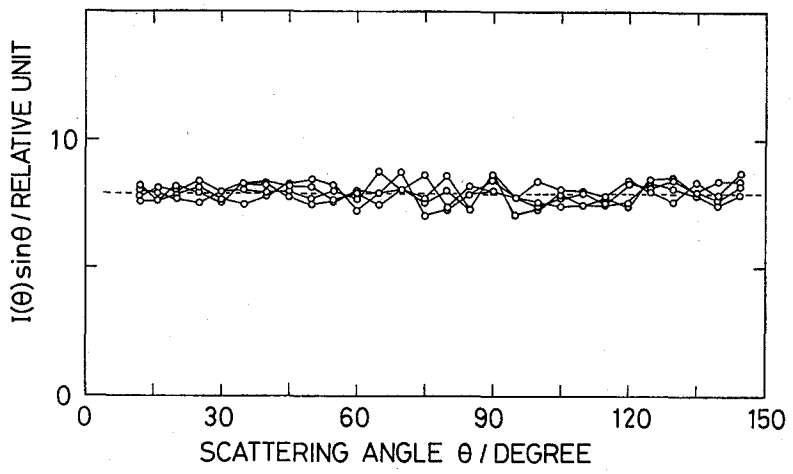

Fig. 5. Angular variation of the scattered light from benzene. The measuring temperature was 25°C and the detector exposure time was 500 ms.

above. 28 peaks in Figure 4 represent the scattered light intensity at 28 angles in the range 12°–145°, from the left to the right. The peak at 145° is not completely shown because the abscissa is limited to 500 channels in this display. The envelope connecting each top of these peaks forms roughly a curve of $(\sin\theta)^{-1}$ with its minimum at 90° (a peak at channel numbers around 300). The integrated peak area at each angle θ is equal to the scattered light intensity at the angle $I(\theta)$. Four zigzag lines in Figure 5, which represent $I(\theta) \times \sin\theta$ vs θ plots, were calculated

from a series of four data ($I(\theta)$ vs channel data) as illustrated in Figure 4. The values are constant to within the deviation $\pm 15\%$. This deviation is fairly large from a classical (static) light scattering point of view. Howevre, this amount was arized mainly from the present data acquisition speed at which the detector was exposured only for 500 ms per one cycle of data acquisition. When the exposure time was extended up to 10 sec, for example, the deviation of $I(\theta) \times \sin\theta$ values from their average decreased down to ± 2-3%, which amount is comparable well with a standard deviation level of usual classical light scattering photometers.[7]

OPTIMUM EXPOSURE TIME OF THE DETECTOR AND LONG TERM STABILIZATION OF THE DETECTOR SENSITIBITY

The present TIDILS system has the faculty of performing data acquisition of 512 channels at the maximum speed of 1 ms, as described already. The system however showed this faculty only when the measuring object emitted strong scattered light intensity. Usual polymer solutions did not scatter light sufficient to allow the system to drive at such a high speed with a stable amounts of signal. We examined a dilute solution of polystyrene in benzene at 25°C in order to settle the proper exposure time of the detector and found out that the optimum exposure time of the detector was more than 12 ms.

Experimental reliability of this TIDILS system depends strongly on long term stability of the detector sensitibity. In other words, the detector sensitibity should be constant during a series of data acquisition cycles made in the experiment in question. The stability is disordered by high voltage fluctuation applied on the image intensifier and by dark signal fluctuation appeared on the detector. The former was little or no, but the latter became sometimes large enough to distort a real signal when weak scattering objects such as benzene were measured. The dark signal fluctuation arose from electric discharge induced randomly in a very narrow gap between the sensitive surface of the image intensifier and the polished edge surface of the fiber holder. The amount of the electric discharge was large in a central portion of the intensifier surface and increased with increasing the voltage applied to the intensifier. However, we could decrease it down to a noise level with a pair of thin films made of high insulation transparent and of metal, both were sandwiched in between the gap. The insulation film suppressed the electric discharge. The metal film, which had a window of just the size of optical fiber holder, made easy to release the electric discharge even if induced, since the film was earthed to ground. Long term stability of the detector was thus assured under applied voltage of 0–1.0 KV.

MEASUREMENTS OF ANGULAR DISTRIBUTION OF THE SCATTERED LIGHT FROM A STYRENE-BUTADIENE DIBLOCK COPOLYMER/n-DECANE SOLUTION

A styrene (S)-butadiene (B) diblock copolymer ($M_n = 6.5 \times 10^4$, 32.4 wt% PS) dissolved in *n*-decane shows various types of structures due to microphase separation, since *n*-decane is a selective solvent for this copolymer; good for the B subchains and presipitant for the S subchains. The structures depend on the polymer concentration and temperature. At the copolymer concentration higher than 2.8 wt% and

at 25°C, the S parts coagurate intermolecularly (the "core") and the B parts surround the core (the "shell"), forming a single micelle or higher order structures composed of the intermiceller aggregation and so on.[8] A 15 wt% solution of the SB copolymer in *n*-decane was very viscous and a clear opalescent blue color, which aspect indicated that some structure was formed in the solution. When illuminated continuously with a strong laser beam, the illuminated part of the solution will be subjected to thermal agitation and the structure in this area will fluctuate with time. The structure will be disordered and disappear as time passes. Contrarily, the structure formation will be observed when the heated solution is plunged into low temperature state.

These two processes mentioned above were examined with the TIDILS system. Figure 6 shows the time dependence of angular distribution of the scattered light intensity from a 15 wt% SB/*n*-decane solution under continuous illumination with

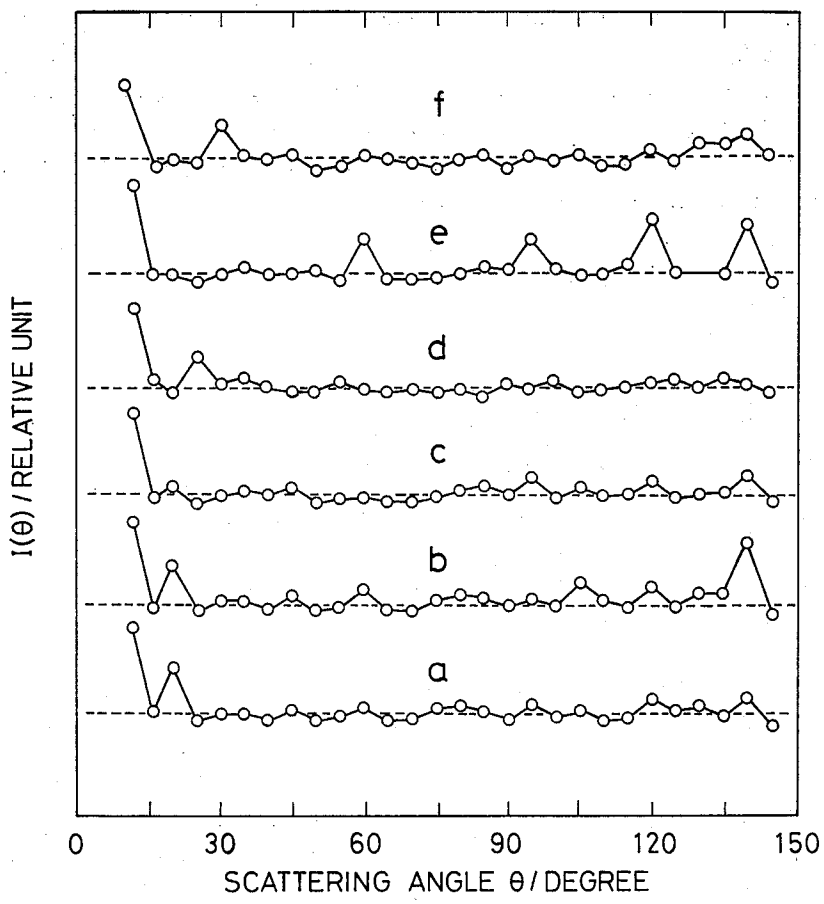

Fig. 6. Time dependent structure change caused by thermal agitation which occuring in a 15 wt% solution of a styrene-butadiene diblock copolymer dissolved in *n*-decane. The scattered light intensity at (a) $t=0$ ms, (b) 160 ms, (c) 480 ms, (d) 1280 ms, (e) 1920 ms, and (f) 320 sec after application of the laser beam to the solution is plotted as a function of the scattering angle in the range 12°–145°. The exposure time of the detector was 100 ms in each experiment.

the incident laser beam. This solution had been prepared about one month before the present measurements. The scattered light from solution was measured at t=0 ms, 160 ms, 480 ms, 1280 ms, 1920 ms, and 320 sec (from the bottom to the top), respectively, after the solution was subjected to the laser beam of 30 mW power. The exposure time of the detector was 100 ms. In the figure, the intensity at θ= 12° (the left end point) was attenuated to 25%. A long-range structure represented by a peak at θ=20° was found to change as fast as 160 ms and rather shift to another structure at θ=25° and to that at θ=30°, disappearing finally. On the other hand, a short-range structures at θ=95°, 120°, and 140° change little and little for several seconds, and these are found to disappear at t=320 sec as illustrated in the sub-figure (f). Figure 7 illustrates the results of a reverse process of Figure 6. Here, a 15 wt% SB/*n*-decane solution was heated up to 60°C for 30 minutes prior to the present measurement and then suddenly cooled down to 17°C. The angular distribution of the scattered light intensity was measured at t=15 sec, 85 sec, and 460 sec (from the bottom to the top), respectively, after the solution was set at 17°C. The detector was exposed for 500 ms at each time. The structure represented at θ=25° begins to grow at t=85 sec but remains unchanged even at t=460 sec. This means that it takes long time to form a structure of longer-range order such as represented by a peak at θ=20° in Figure 6.

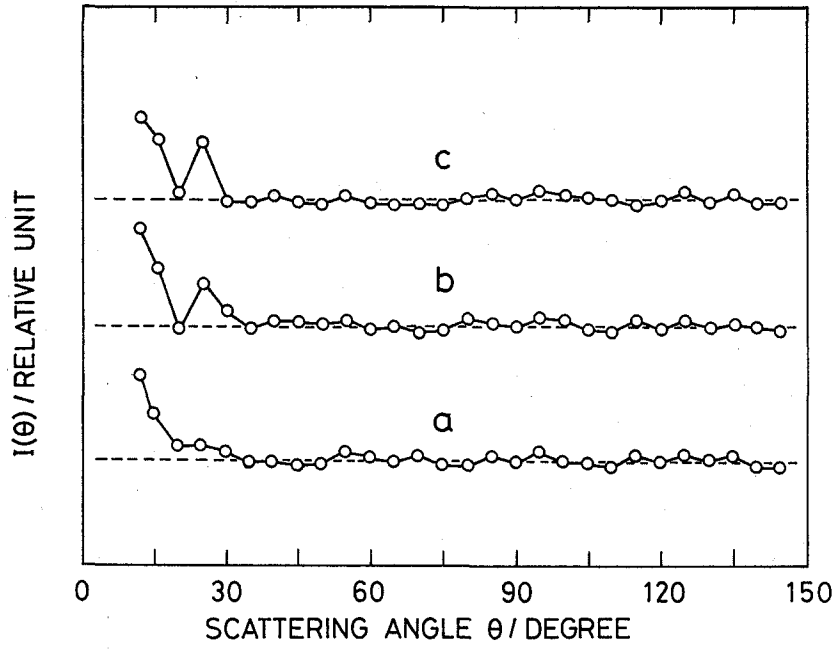

Fig. 7. Time dependent structure formation caused by temperature drop from 60°C to 17°C in a 15 wt% solution of a styrene-butadiene diblock copolymer in *n*-decane. The scattered light intensity is plotted against the angle at (a) 15 sec, (b) 85 sec, and (c) 460 sec after the solution was plunged into circumstances at 17C°. The exposure time of the detector was 500 ms.

ACKNOWLEDGMENTS

The authors are very grateful to Messrs. Kichizo Oono, Kiyomitsu Tanno, and Katsumi Imanishi of the machine shop in this institute, who made appropriate advice and careful mechanical work. Dr. Masukazu Hirata assisted us in our work of the inspection of the TIDILS system and of data processing made on the computer; this is acknowledged gratefully.

REFERENCES AND NOTES

(1) To whom correspondence should be addressed.
(2) Y. Tsunashima, N. Nemoto, and M. Kurata, Shiken Kenkyu (Grant from the Ministry of Education, Science and Culture) Report on "Time-Division Integrated Light Scattering Spectroscopy: Studies on Growing Processes of Higher Order Structures in Block Copolymer Solutions", (Japanese) March, 1987.
(3) H. Utiyama and Y. Tsunashima, *Appl. Opt.* **9,** 1330 (1970).
(4) Similar idea on this structure has already been reported in refs. 3 and 5.
(5) B.H. Zimm, *J. Chem. Phys.* **16,** 1099 (1948). W.B. Dandliker and J. Kraut, *J. Am. Chem. Soc.* **78,** 2380 (1956).
(6) M. Born and E. Wolf, "Principles of Optics", 4th Ed., Pergamon, Oxford, 1970.
(7) M.B. Huglin (Ed), "Light Scattering from Polymer Solutions", Academic Press, London, 1972. P. Kratochvil, "Classical Light Scattering from Polymer Solutions", chapter 2, Elsevier Science Pub., N.Y., 1987. Y. Tsunashima, M. Hirata, N. Nemoto, and M. Kurata, *Macromolecules* **21,** 1107 (1988).
(8) Y. Tsunashima, M. Hirata, and Y. Kawamata, *Macromolecules,* in press.